PHYSICAL REVIEW D **87,** 055004 (2013)

Little Higgs theory confronted with the LHC Higgs data

Xiao-Fang Han,[1] Lei Wang,[1] Jin Min Yang,[2] and Jingya Zhu[2]

[1]*Department of Physics, Yantai University, Yantai 264005, People's Republic of China*

[2]*State Key Laboratory of Theoretical Physics, Institute of Theoretical Physics, Academia Sinica, Beijing 100190, People's Republic of China*

(Received 1 February 2013; published 5 March 2013)

We confront the little Higgs theory with the LHC Higgs search data (up to 17 fb^{-1} of the combined 7 and 8 TeV run). Considering some typical models, namely, the littlest Higgs model, the littlest Higgs model with T parity (LHT-A and LHT-B), and the simplest little Higgs model, we scan over the parameter space in the region allowed by current experiments. We find that in these models the inclusive and exclusive (via gluon-gluon fusion) diphoton and ZZ^* signal rates of the Higgs boson are always suppressed and approach the standard model predictions for a large-scale f. Thus, the ZZ^* signal rate is within the 1σ range of the experimental data while the inclusive diphoton signal rate is always outside the 2σ range. Especially, in the LHT-A the diphoton signal rate is outside the 3σ range of the experimental data for $f < 800$ GeV. We also perform a global χ^2 fit to the available LHC and Tevatron Higgs data, and find that these models provide no better global fit to the whole data set (only for some special channels a better fit can be obtained, especially in the LHT-B).

DOI: 10.1103/PhysRevD.87.055004 PACS numbers: 14.80.Ec, 12.60.Fr, 14.70.Bh

I. INTRODUCTION

To solve the fine-tuning problem of the standard model (SM), the little Higgs theory [1] is proposed as a kind of electroweak symmetry breaking mechanism accomplished by a naturally light Higgs sector. So far various realizations of the little Higgs have been proposed [2–4], which can be categorized generally into two classes [5]. One class utilizes some product group, represented by the littlest Higgs (LH) model [3] in which the SM $SU(2)_L$ gauge group is from the diagonal breaking of two (or more) gauge groups. Further, to relax the constraints from the electroweak precision data [6], a discrete symmetry called T parity is introduced to the LH [7,8]. The LH with T parity (LHT) can provide a candidate for the cosmic dark matter. The other class uses some simple group, represented by the simplest little Higgs (SLH) model [4] in which a single large gauge group is broken down to the SM $\text{SU}(2)_L$. Since these little Higgs models predict different Higgs property from the SM prediction, they can be tested in the Higgs search experiments.

Recently, the CMS and ATLAS collaborations have announced the observation of a new boson around 125 GeV [9,10]. This observation is corroborated by the Tevatron search results which showed a 2.5σ excess in the range 115–135 GeV [11]. The LHC search results have just been updated by using 17 fb^{-1} of 7 and 8 TeV data [12–16]. We note that for the inclusive data, the signal rates of ZZ^* and WW^* are consistent with the SM values while the diphoton rate is sizably higher than the SM expectation. For the $Vb\bar{b}$ and $\tau\bar{\tau}$ channels, the uncertainties are still large.

Although so far the inclusive Higgs search data are roughly consistent with the SM predictions, the diphoton enhancement has been explained in various new physics models, such as the supersymmetry models [17], the two-Higgs-doublet models [18], the Higgs triplet model [19], the models with extra dimensions [20], and other extensions of Higgs models [21]. For the little Higgs theory, the Higgs property (especially the diphoton decay) was thoroughly studied even before the LHC Higgs data [22–25]. In this work we use the latest LHC Higgs data to check the status of the little Higgs theory. For this purpose, we will examine some typical models, namely, the LH, the littlest Higgs model with T parity (LHT-A and LHT-B), and the SLH. The model predictions for the Higgs signal rates will be compared with the experimental data. Also we will perform a global χ^2 fit to the available LHC and Tevatron Higgs data [26] to figure out if the little Higgs theory can provide a better fit than the SM. Besides, we will show the Higgs couplings and some exclusive signal rates in comparison with the Higgs data as well as the SM predictions.

Our work is organized as follows. In Sec. II we recapitulate the little Higgs models. In Sec. III we confront the model predictions for the Higgs signal rates with the experimental data. Finally, we give our conclusion in Sec. IV.

II. LITTLE HIGGS MODELS

A. Littlest Higgs model

The LH model [3] consists of a nonlinear sigma model with a global $SU(5)$ symmetry which is broken down to $SO(5)$ by a vacuum expectation value (vev) f. A subgroup $[SU(2) \otimes U(1)]^2$ of $SU(5)$ is gauged. The heavy gauge bosons (W_H, Z_H, A_H), triplet scalar (Φ^{++}, Φ^{+}, Φ^{0}, Φ^{P}), and top quark partner T quark are, respectively, introduced

to cancel the Higgs mass one-loop quadratic divergence contributed by the gauge bosons, Higgs boson, and top quark of the SM. There masses are given as

$$m_{Z_H} = m_{W_H} = \frac{gf}{2sc}, \qquad m_{A_H} = \frac{g'f}{2\sqrt{5}s'c'},$$
$$m_\Phi = \frac{\sqrt{2}m_h}{\sqrt{1-x^2}}\frac{f}{v}, \qquad m_T = \frac{m_t f}{s_t c_t v}, \tag{1}$$

where h and v are, respectively, the SM-like Higgs boson and its vev, c, $s \equiv \sqrt{1-c^2}$, c', and $s' \equiv \sqrt{1-c'^2}$ are the mixing parameters in the gauge boson sector, x is a free parameter of the Higgs sector proportional to the triplet vev v' defined as $x = 4fv'/v^2$, and c_t and $s_t \equiv \sqrt{1-c_t^2}$ are the mixing parameters between t and T.

The relevant Higgs couplings are given as [23,24]

$$\begin{aligned}\mathcal{L} = {} & 2\frac{m_{W_H}^2}{v} y_{W_H} W_H^+ W_H^- h + 2\frac{m_W^2}{v} y_W W^+ W^- h \\ & + 2\frac{m_Z^2}{v} y_Z ZZh - 2\frac{m_\Phi^2}{v} y_{\Phi^+}\Phi^+\Phi^- h \\ & - 2\frac{m_\Phi^2}{v} y_{\Phi^{++}}\Phi^{++}\Phi^{--}h, \qquad -\frac{m_T}{v} y_T \bar{T}Th \\ & - \frac{m_t}{v} y_t \bar{t}th - \frac{m_f}{v} y_f \bar{f}fh(f = b, \tau)\end{aligned} \tag{2}$$

with

$$\begin{aligned} y_{W_H} &= -s^2c^2\frac{v^2}{f^2}, \\ y_W &= 1 + \frac{v^2}{f^2}\left[-\frac{1}{6} - \frac{1}{4}(c^2-s^2)^2\right] \\ &= 1 + \frac{v^2}{f^2}\left[-\frac{5}{12} + c^2s^2\right], \\ y_Z &= 1 + \frac{v^2}{f^2}\left[-\frac{1}{6} - \frac{1}{4}(c^2-s^2)^2 - \frac{5}{4}(c'^2-s'^2) + \frac{1}{4}x^2\right], \\ y_{\Phi^+} &= \frac{v^2}{f^2}\left[-\frac{1}{3} + \frac{1}{4}x^2\right], \\ y_{\Phi^{++}} &= \frac{v^2}{f^2}\mathcal{O}\left(\frac{x^2}{16}\frac{v^2}{f^2}, \frac{1}{16\pi^2}\right), \qquad y_T = -c_t^2 s_t^2 \frac{v^2}{f^2}, \\ y_t &= 1 + \frac{v^2}{f^2}\left[-\frac{2}{3} + \frac{x}{2} - \frac{x^2}{4} + c_t^2 s_t^2\right], \\ y_{b,\tau} &= 1 + \frac{v^2}{f^2}\left[-\frac{2}{3} + \frac{x}{2} - \frac{x^2}{4}\right]. \end{aligned} \tag{3}$$

The heavy top partner quark, gauge boson, and triplet scalar give the contributions to $h \to gg$ and $h \to \gamma\gamma$ at one-loop level. Their contributions are sensitive to y_T, y_{W_H}, y_{Φ^+}, and $y_{\Phi^{++}}$, and not sensitive to the actual values of their masses as long as they are much larger than half of the Higgs boson mass. Further, the factors y_T, y_{W_H}, and y_{Φ^+} are at the order of $\frac{v^2}{f^2}$, and thus the next-to-leading order masses of these charged particles will contribute to the three factors at an order higher than $\frac{v^2}{f^2}$ [see Eq. (2)], which are ignored in our calculations. Since the $h\Phi^{++}\Phi^{--}$ coupling is very small, the contributions of the doubly charged scalar to the effective $h\gamma\gamma$ coupling can be ignored.

In the LH model the relation between G_F and v is modified from its SM form, such that [24]

$$v \simeq v_{\rm SM}\left[1 - \frac{v_{\rm SM}^2}{f^2}\left(-\frac{5}{24} + \frac{1}{8}x^2\right)\right], \tag{4}$$

where $v_{\rm SM} = 246$ GeV is the SM Higgs vev.

B. Littlest Higgs models with T parity

T parity requires that the coupling constant of $SU(2)_1$ $[U(1)_1]$ equals that of $SU(2)_2$ $[U(1)_2]$, which leads to that the four mixing parameters in gauge sector c, s, c', and s' are equal to $1/\sqrt{2}$, respectively. Under T parity, the SM bosons are T-even and the new bosons are T-odd. Therefore, the coupling $H^\dagger \phi H$ is forbidden, leading to the triplet vev $v' = 0$ and $x = 0$. Since the correction of W_H to the relation between G_F and v is forbidden by T parity, the Higgs vev v is different from that of the LH [25], which is

$$v \simeq v_{\rm SM}\left(1 + \frac{1}{12}\frac{v_{\rm SM}^2}{f^2}\right). \tag{5}$$

Taking $c = s = c' = s' = 1/\sqrt{2}$ and $x = 0$, we can obtain the Higgs couplings to the gauge bosons and scalars of the LHT from Eqs. (2) and (3).

For each SM quark (lepton), a heavy vectorlike quark (lepton) with a T-odd quantum number is added in order to preserve T parity. The Higgs couplings to each generation of mirror quarks are given by [25]

$$\begin{aligned}\mathcal{L}_\kappa \simeq {} & -\sqrt{2}\kappa f\left[\frac{1+c_\xi}{2}\bar{u}_{L_-}u'_R - \frac{1-c_\xi}{2}\bar{u}_{L_-}q_R - \frac{s_\xi}{\sqrt{2}}\bar{u}_{L_-}\chi_R\right] \\ & - m_q\bar{q}_L q_R - m_\chi \bar{\chi}_L\chi_R + \text{H.c.}\end{aligned} \tag{6}$$

with $c_\xi \equiv \cos\frac{v+h}{\sqrt{2}f}$ and $s_\xi \equiv \sin\frac{v+h}{\sqrt{2}f}$. After diagonalization of the mass matrix in Eq. (6), we can get the T-odd mass eigenstates u_-, q, and χ as well as their couplings to the Higgs boson.

For the implementation of T parity in the Yukawa sector of the top quark, the T-parity image for the original top quark interaction of the LH is introduced to make the Lagrangian T-invariant [25,27],

$$\begin{aligned}\mathcal{L}_t \simeq {} & -\lambda_1 f\left[\frac{s_\Sigma}{\sqrt{2}}\bar{u}_{L_+}u_R + \frac{1+c_\Sigma}{2}\bar{U}_{L_+}u_R\right] \\ & - \lambda_2 f\bar{U}_{L_+}U_{R_+} + \text{H.c.}\end{aligned} \tag{7}$$

with $c_\Sigma \equiv \cos\frac{\sqrt{2}(v+h)}{f}$ and $s_\Sigma \equiv \sin\frac{\sqrt{2}(v+h)}{f}$. The mass eigenstates t and T can be obtained by mixing the interaction eigenstates in Eq. (7). The mixing parameters and couplings are the same as those in the LH when the value of x is taken to be 0, which are

$$r = \frac{\lambda_1}{\lambda_2}, \qquad c_t = \frac{r}{\sqrt{r^2+1}}, \qquad s_t = \frac{1}{\sqrt{1+r^2}}. \quad (8)$$

For the SM down-type quarks (leptons), the Higgs couplings of LHT have two different cases [25]:

$$\frac{C_{hd\bar{d}}}{C^{\rm SM}_{hd\bar{d}}} \simeq 1 - \frac{1}{4}\frac{v^2_{\rm SM}}{f^2} + \frac{7}{32}\frac{v^4_{\rm SM}}{f^4} \quad \text{for LHT-A,}$$
$$\simeq 1 - \frac{5}{4}\frac{v^2_{\rm SM}}{f^2} - \frac{17}{32}\frac{v^4_{\rm SM}}{f^4} \quad \text{for LHT-B.}$$

The relation of down-type quark couplings also applies to the lepton couplings.

C. Simplest little Higgs model

The SLH [4] model has an $[SU(3)\times U(1)_X]^2$ global symmetry. The gauge symmetry $SU(3)\times U(1)_X$ is broken down to the SM electroweak gauge group by two copies of scalar fields Φ_1 and Φ_2, which are triplets under the $SU(3)$ with aligned vevs f_1 and f_2.

The new heavy charged gauge boson $W'^{\pm}$ can contribute to the effective $h\gamma\gamma$ coupling. The Higgs couplings to $W'W'$, WW, and ZZ are given by [28]

$$\mathcal{L} = 2\frac{m^2_{W'}}{v} y_{W'} W'^{+}W'^{-}h + 2\frac{m^2_W}{v} y_W W^+W^-h + 2\frac{m^2_Z}{v} y_Z ZZh, \quad (9)$$

where

$$m^2_{W'^+} = \frac{g^2}{2}f^2, \quad (10)$$

$$y_{W'} \simeq -\frac{v^2}{2f^2}, \quad (11)$$

$$y_W \simeq \frac{v}{v_{\rm SM}}\left[1 - \frac{v^2_{\rm SM}}{4f^2}\frac{t^4_\beta - t^2_\beta + 1}{t^2_\beta}\right], \quad (12)$$

$$y_Z \simeq \frac{v}{v_{\rm SM}}\left[1 - \frac{v^2_{\rm SM}}{4f^2}\left(\frac{t^4_\beta - t^2_\beta + 1}{t^2_\beta} + (1-t^2_W)^2\right)\right] \quad (13)$$

with $f = \sqrt{f_1^2 + f_2^2}$, $t_\beta \equiv \tan\beta = f_2/f_1$, $c_\beta = f_1/f$, $s_\beta = f_2/f$, and $t_W = \tan\theta_W$.

The gauged $SU(3)$ symmetry promotes the SM fermion doublets into $SU(3)$ triplets. The Higgs interactions with the quarks are given by [29]

$$\mathcal{L}_t \simeq -f\lambda_2^t[x^t_\lambda c_\beta t_1^{c'}(-s_1 t'_L + c_1 T'_L) + s_\beta t_2^{c'}(s_2 t'_L + c_2 T'_L)] + \text{H.c.}, \quad (14)$$

$$\mathcal{L}_d \simeq -f\lambda_2^d[x^d_\lambda c_\beta d_1^{c'}(s_1 d'_L + c_1 D'_L) + s_\beta d_2^{c'}(-s_2 d'_L + c_2 D'_L)] + \text{H.c.}, \quad (15)$$

$$\mathcal{L}_s \simeq -f\lambda_2^s[x^s_\lambda c_\beta s_1^{c'}(s_1 s'_L + c_1 S'_L) + s_\beta s_2^{c'}(-s_2 s'_L + c_2 S'_L)] + \text{H.c.}, \quad (16)$$

where

$$s_1 \equiv \sin\frac{t_\beta(h+v)}{\sqrt{2}f}, \qquad s_2 \equiv \sin\frac{(h+v)}{\sqrt{2}t_\beta f}. \quad (17)$$

After diagonalization of the mass matrix in Eqs. (14)–(16), we can get the mass eigenstates (t, T), (d, D), and (s, S) as well as their couplings to the Higgs boson.

The Higgs couplings to $b\bar{b}$ and $\tau\tau$ normalized to the SM values are

$$\frac{C_{hb\bar{b}}}{C^{\rm SM}_{hb\bar{b}}} = \frac{C_{h\tau\tau}}{C^{\rm SM}_{h\tau\tau}} \simeq \frac{v_{\rm SM}}{v}\left[1 - \frac{1}{6s^2_\beta c^2_\beta}\frac{v^2}{f^2}\right]. \quad (18)$$

The SLH model predicts a pseudoscalar η, which obtains the mass via a tree-level μ term,

$$-\mu^2(\Phi_1^\dagger\Phi_2 + \text{H.c.}) = -2\mu^2 f^2 s_\beta c_\beta \cos\left(\frac{\eta}{\sqrt{2}s_\beta c_\beta f}\right)\cos\left(\frac{\sqrt{H^\dagger H}}{f c_\beta s_\beta}\right) \quad (19)$$

with H being the SM-like Higgs doublet field.

In the SLH, the relation between G_F and v is modified from its SM form, which can induce [28]

$$v \simeq v_{\rm SM}\left[1 + \frac{v^2_{\rm SM}}{12f^2}\frac{t^4_\beta - t^2_\beta + 1}{t^2_\beta} - \frac{v^4_{\rm SM}}{180f^4}\frac{t^8_\beta - t^6_\beta + t^4_\beta - t^2_\beta + 1}{t^4_\beta}\right]. \quad (20)$$

III. HIGGS PROPERTIES CONFRONTED WITH THE HIGGS DATA

A. Calculations

As an effective theory, the Higgs potential of little Higgs models is affected by the theory at the cutoff scale [30]. We assume that there are large direct contributions to the potential from the physics at the cutoff, so that the constraints of Higgs mass on the parameter space of the little Higgs models are loosened greatly. In our calculations, the Higgs mass is fixed as 125.5 GeV. We consider the relevant QCD and electroweak corrections using the code Hdecay [31]. For the Higgs productions and decays, the little Higgs models give the corrections by directly

modifying the Higgs couplings to the relevant SM particles.

For the loop-induced decays $h \to gg$ and $h \to \gamma\gamma$, the little Higgs models give the partial corrections via the reduced $ht\bar{t}$ and hWW couplings, respectively. Besides, $h \to gg$ can get contributions from the loops of heavy partner quark T in the LH, T, and T-odd quarks in the LHT, and T, D, and S in the SLH. In addition to the loops of the heavy quarks involved in the $h \to gg$, the decay $h \to \gamma\gamma$ can be also altered by the loops of W_H, Φ^+, Φ^{++} in the LH and LHT and by W' in the SLH. Note that the LHT and SLH also predict some neutral heavy neutrinos, which do not contribute to the $h\gamma\gamma$ coupling at the one-loop level. Although the charged heavy leptons are predicted by the LHT, they do not have direct couplings with the Higgs boson.

In the LH the new free parameters are f, c, c', c_t, and x. We scan over these parameters in the ranges

$$1\ \text{TeV} < f < 3.5\ \text{TeV}, \quad 0 < c < 1, \quad 0 < c' < 1, \quad 0.45 < c_t < 0.9, \quad 0 < x < 1. \tag{21}$$

In the LHT, the new T-odd quarks can give the additional contributions to the $h \to gg$ and $h \to \gamma\gamma$ via the loops, which are not sensitive to the actual values of their masses as long as they are much larger than half of the Higgs boson mass. The parameters $c = s = c' = s' = 1/\sqrt{2}$ and $x = 0$ are fixed by T parity. T parity can relax the constraints of the electroweak precision data sizably, leading to a scale f as low as 500 GeV [32]. In our calculation we scan f in the range of 0.5–3.5 TeV.

In the LH and LHT, the parameter c_t determines the Higgs couplings to t, T, and m_T, and is involved in the calculations of the $h \to gg$ and $h \to \gamma\gamma$. The c_t dependence of the top quark loop and T quark loop can cancel each other to a large extent [see Eq. (3)]. The electroweak precision data favor $0.5 \le r \le 2.0$, which leads to $0.45 < c_t < 0.9$ [32]. Besides, for the LH, the c and s dependence of the W_H loop and W loop in the $h \to \gamma\gamma$ decay can cancel each other to some extent [see Eq. (3)]. The parameter x can affect $\sigma(gg \to h)$ and $\Gamma(h \to b\bar{b})$, but the effects of x on $\sigma(gg \to h)/\Gamma(h \to b\bar{b})$ are weakened to a large extent [see Eq. (3)]. For $m_h = 125.5$ GeV, the decay $h \to A_H A_H$ is kinematically forbidden in the LH and LHT.

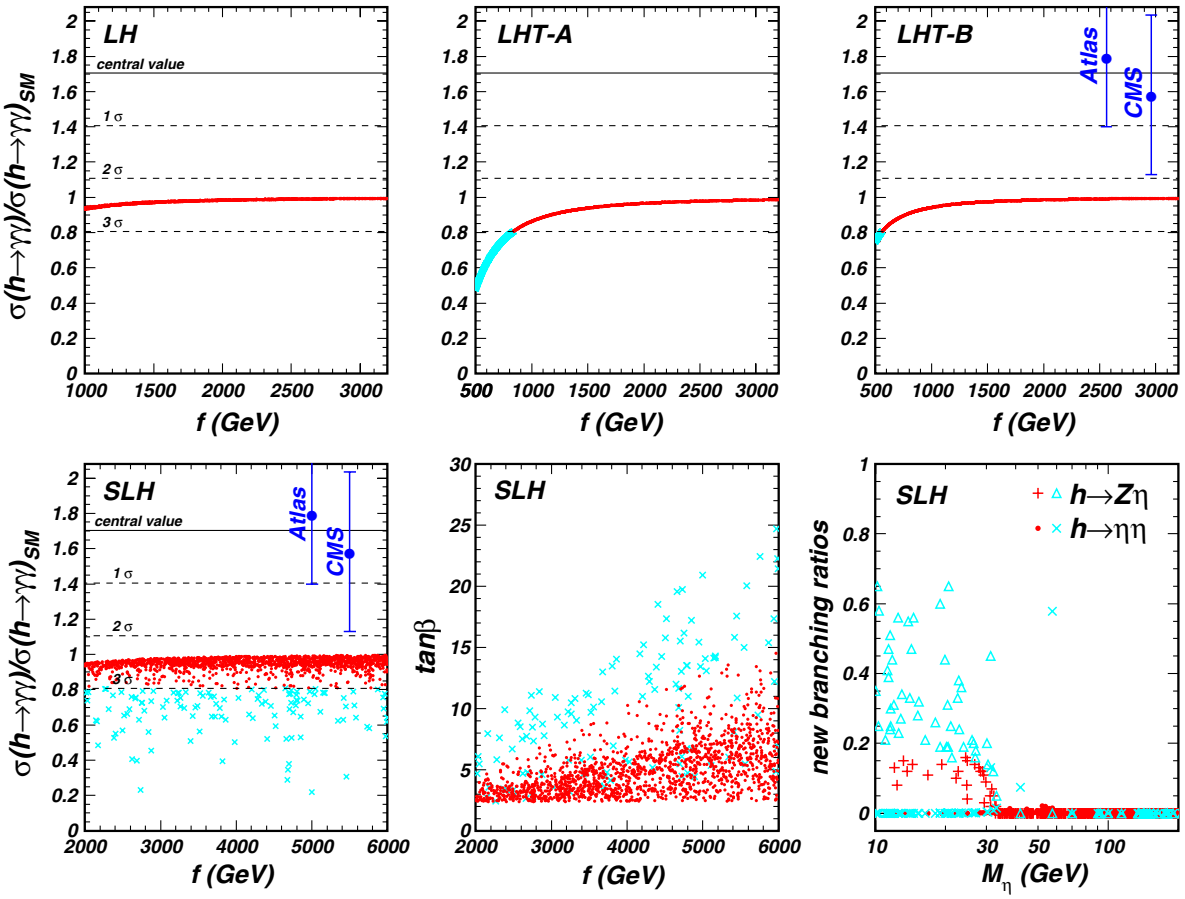

FIG. 1 (color online). The scatter plots of the parameter space projected on the planes of the LHC diphoton rate versus f, $\tan\beta$ versus f, and the branching ratios of $h \to Z\eta$ and $h \to \eta\eta$ versus m_η. The bullets and pluses (red) are within the 3σ range of the experimental data of the inclusive diphoton rate, while the crosses and triangles (sky blue) are outside the 3σ.

In the SLH, we take f, t_β, m_T, m_D, m_S, and m_η as new free parameters. Reference [4] shows that the LEP-II data require $f > 2$ TeV. Here, we assume the new flavor mixing matrices in lepton and quark sectors are diagonal [5,33] so that f and t_β are free from the experimental constraints of the lepton and quark flavor violating processes. Besides, the contributions to the electroweak precision data can be suppressed by a large t_β [4,34]. For the perturbation to be valid, t_β cannot be too large for a fixed f. We require $\mathcal{O}(v_0^4/f^4)/\mathcal{O}(v_0^2/f^2) < 0.1$ in the expansion of v. The small masses of the d quark and s quark require that x_λ^d and x_λ^s are very small. So there are almost no mixings between the SM down-type quarks and their heavy partners, and the results are not sensitive to m_D and m_S. In addition to the SM-like decays, the new decays $h \to \eta\eta$ and $h \to Z\eta$ are open for a light enough η, whose partial widths are given by

$$\Gamma(h \to \eta\eta) = \frac{\lambda'^2}{8\pi}\frac{v^2}{m_h}\sqrt{1 - x_\eta}, \tag{22}$$

$$\Gamma(h \to Z\eta) = \frac{m_h^3}{32\pi f^2}\left(t_\beta - \frac{1}{t_\beta}\right)^2 \lambda^{3/2}\left(1, \frac{m_Z^2}{m_h^2}, \frac{m_\eta^2}{m_h^2}\right), \tag{23}$$

where $\lambda' = -m_\eta^2/[4f^2 s_\beta^2 c_\beta^2 \cos(v/\sqrt{2}f s_\beta c_\beta)]$, $x_\eta = 4m_\eta^2/m_h^2$, and $\lambda(1, x, y) = (1 - x - y)^2 - 4xy$. The constraint from the nonobservation in the decay $\Upsilon \to \gamma\eta$ excludes η with a mass below 5–7 GeV [35]. So we scan over the following parameter space:

$$\begin{aligned} &2\ \text{TeV} < f < 6\ \text{TeV}, \qquad 0.5\ \text{TeV} < m_T < 3\ \text{TeV}, \\ &0.5\ \text{TeV} < m_D(m_S) < 3\ \text{TeV}, \qquad 1 < t_\beta < 30, \\ &10\ \text{GeV} < m_\eta < 500\ \text{GeV}. \end{aligned} \tag{24}$$

B. Numerical results and discussions

The diphoton and ZZ^* are the cleanest channels for the Higgs boson. We show their inclusive signal rates normalized to the SM values in Figs. 1 and 2, respectively.

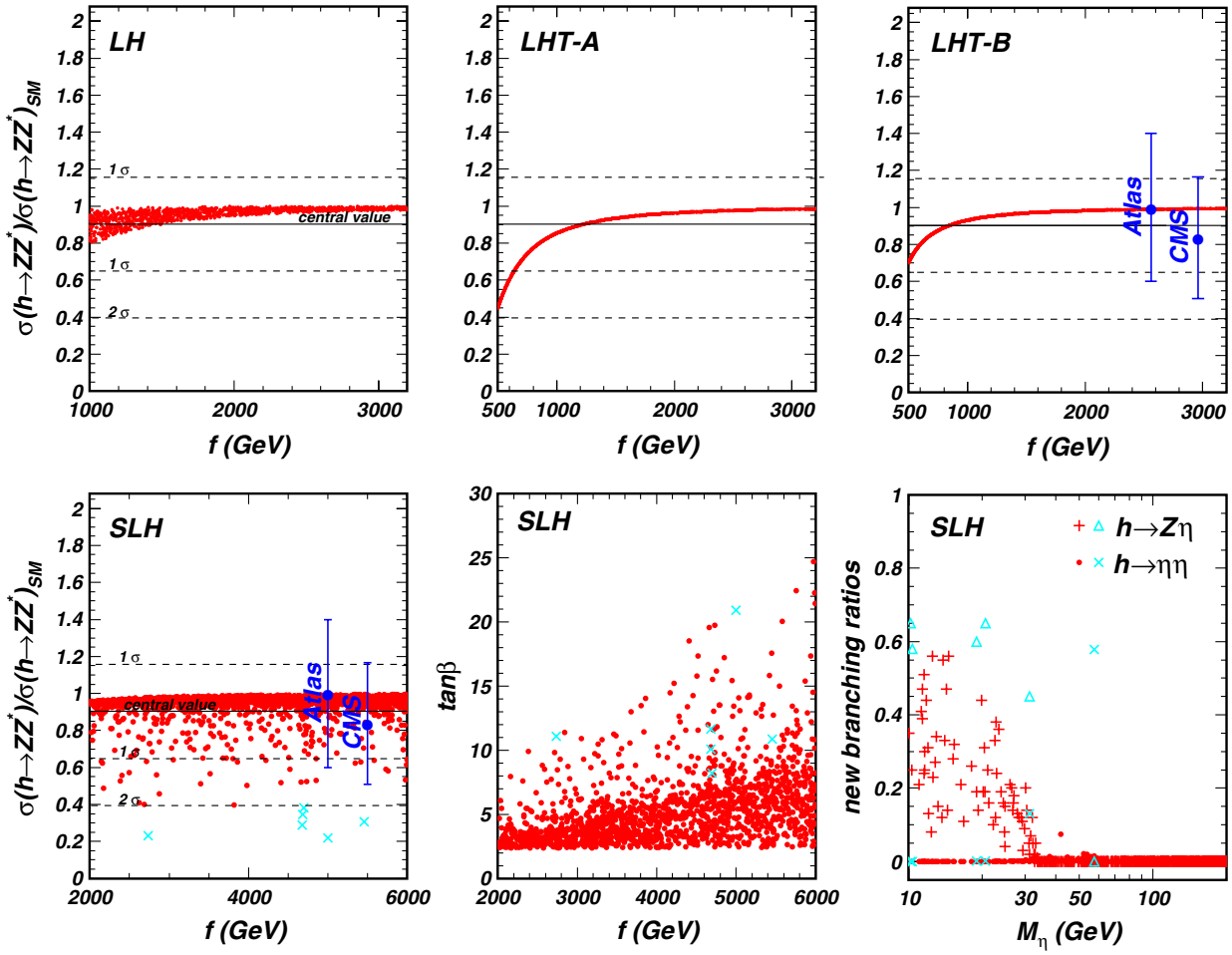

FIG. 2 (color online). Same as Fig. 1, but showing the $pp \to h \to ZZ^* \to 4\ell$ signal rate at the LHC. The bullets and pluses (red) are within the 2σ range of the experimental data of the inclusive ZZ^* rate, while the crosses and triangles (sky blue) are outside the 2σ.

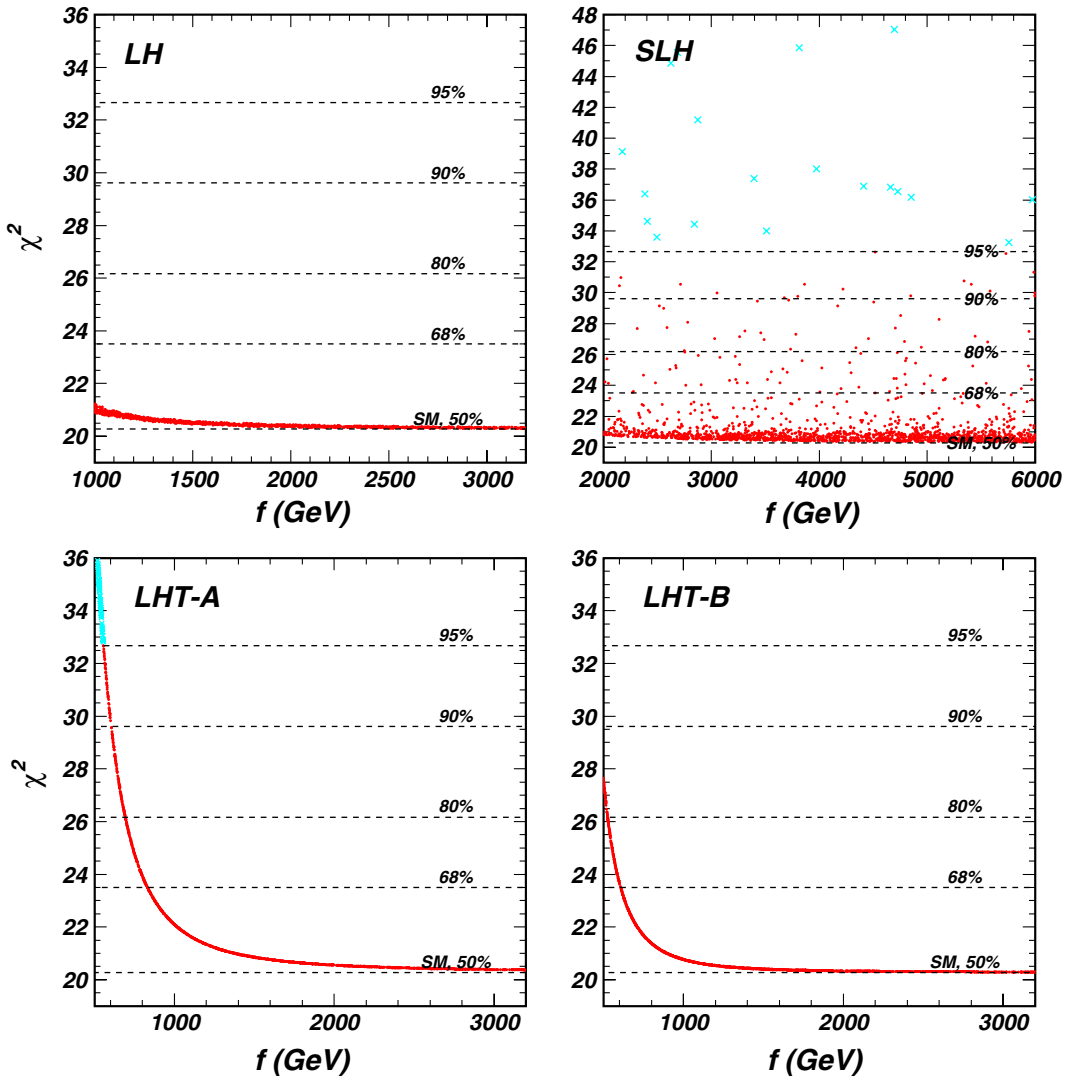

FIG. 3 (color online). The scatter plots of the parameter space projected on the plane of χ^2 versus f. The bullets (red) and crosses (sky blue) denote, respectively, the samples within and beyond 95% confidence level. In calculating χ^2 we use the data of 21 channels [26].

The experimental data come from Ref. [12] for ATLAS and Ref. [13] for CMS. In combining the data of the two collaborations, we assume they are independent and Gaussian distributed. Figures 1 and 2 show that the rates for the two signals in the little Higgs models are always suppressed, and approach the SM predictions for a large-scale f.

For the diphoton channel, in these models the signal rates are always outside the 2σ range of the experimental data. Especially, in the LHT-A the rate is outside the 3σ range for $f < 800$ GeV. In the SLH the diphoton rate is also sensitive to $\tan\beta$ and the data favor a small $\tan\beta$. The value of m_η can be as low as 10 GeV, and the total branching ratio of $h \to Z\eta$ and $h \to \eta\eta$ can only reach 15% to make the diphoton rate within the 3σ range.

For the ZZ^* channel, these models can fit the LHC experimental data quite well. The signal rate can equal to the central value of the experimental data for 1 TeV $< f <$ 1.6 TeV in the LH, $f = 1.2$ TeV in the LHT-A, $f = 0.8$ TeV in the LHT-B, and 2 TeV $< f <$ 6 TeV in the SLH. For the LH, LHT-A, and LHT-B, the rate of ZZ^* is always within the 2σ range of the experimental data in the ranges of parameters scanned. For the SLH, only the parameter space where the total branching ratio of $h \to Z\eta$ and $h \to \eta\eta$ is larger than 60% is disfavored.

Now we perform a global χ^2 fit to the available LHC and Tevatron Higgs data in these little Higgs models. We compute the χ^2 values by the method introduced in Refs. [36,37] with the experimental data of 21 channels from Ref. [26], which are shown in Fig. 7. We assume that the data from different collaborations or for different inclusive search channels are independent of each other. However, the data for different exclusive search channels

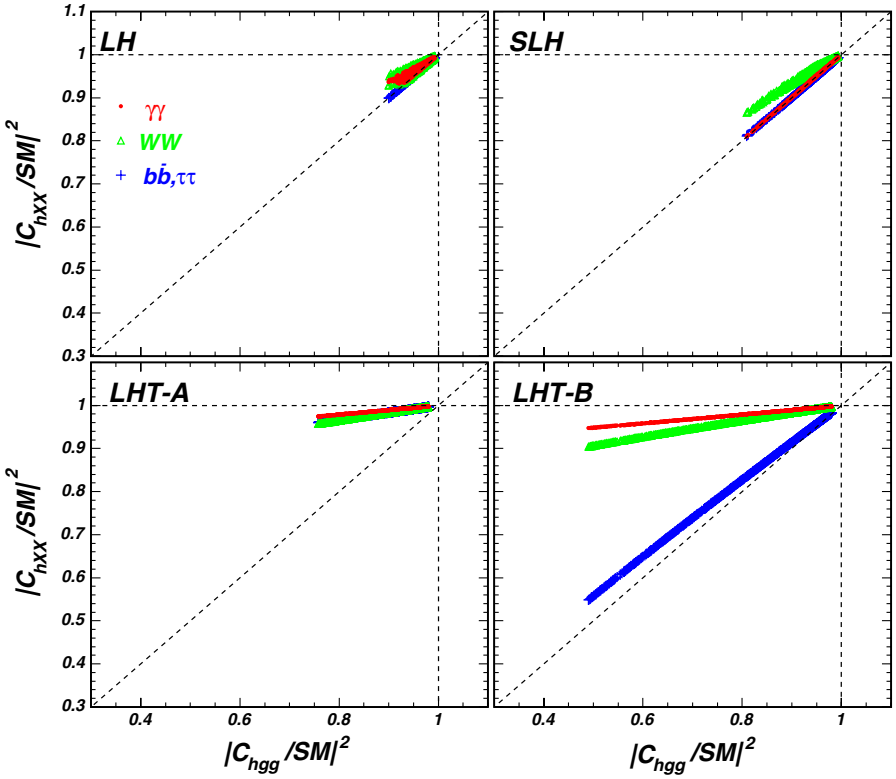

FIG. 4 (color online). The scatter plots of the parameter space showing the Higgs couplings normalized to the SM values. These samples satisfy the conditions (i) within the 3σ range of the diphoton data, (ii) within the 2σ range of the ZZ^* data, (iii) $\chi^2 \leq 32.7$ (corresponding to 95% C.L.).

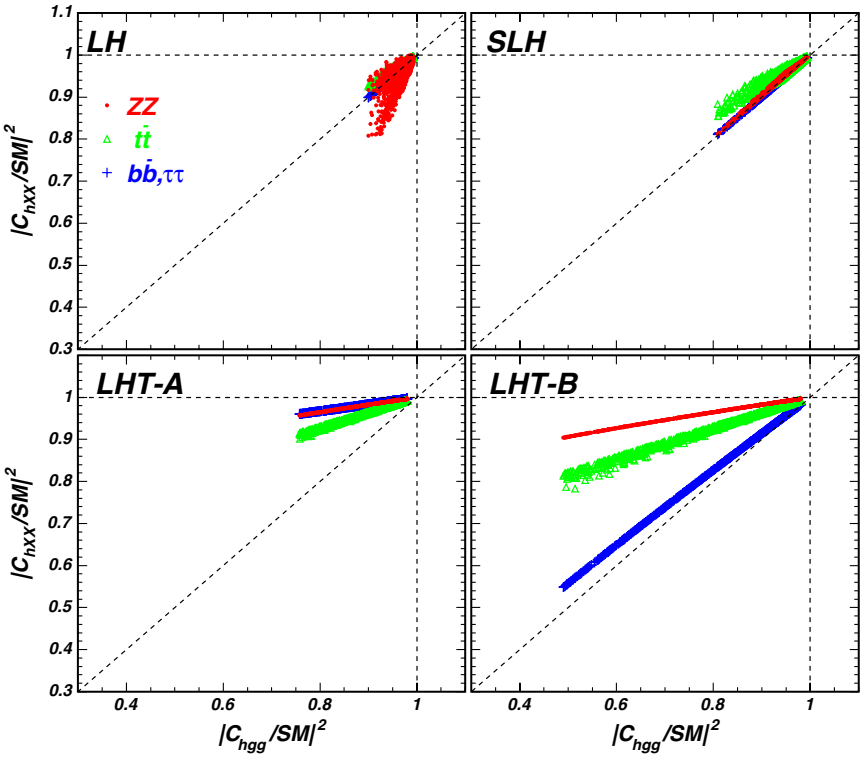

FIG. 5 (color online). Same as Fig. 4, but showing different couplings.

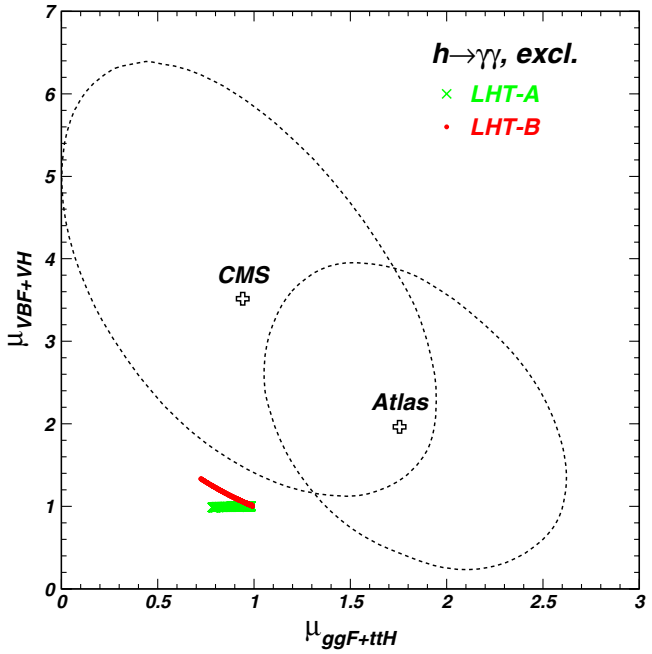

FIG. 6 (color online). The scatter plots of the parameter space in the LHT-A and LHT-B, showing the exclusive diphoton rates from the $VBF + VH$ and $ggF + t\bar{t}H$ channels. The central values and 1σ contours of the LHC experiment are taken from Refs. [13,14].

presented by one collaboration are not independent, and we use the correlation coefficient given in Ref. [26]. For the ATLAS $h \to ZZ^*$ data, since the observed resonance is peaked at $m_h = 123.5$ GeV [15] (different from that of the diphoton data at more than the 2σ level), we follow [15,26] to interpret this data as a 125 GeV Higgs with $\mu(ZZ) = 1.15^{+0.53}_{-0.48}$. A 125 GeV Higgs with such a ZZ^* signal rate can fit the ATLAS ZZ^* data when combined with the background. For a detailed description, see Refs. [15,26].

In Fig. 3 we project these samples on the plane of χ^2 versus f. We see that the χ^2 values of these models are larger than the SM value and approach the SM value for a sufficiently large f (larger than 2, 3, 1.6, and 3 TeV for the LH, LHT-A, LHT-B, and SLH, respectively). Especially, in the LHT-A the value of χ^2 is larger than 32.7 for $f < 530$ GeV, which implies that $f < 530$ GeV is excluded at 95% confidence level from an experimental viewpoint.

Figures 4 and 5 show the Higgs couplings normalized to the SM values. We see that in these little Higgs models the Higgs couplings are all suppressed, and approach the SM values for a large f. The correlations between the couplings are also interesting and may be useful for distinguishing different models. For example, the value of $|C_{hgg}/\mathrm{SM}|/|C_{hb\bar{b}}/\mathrm{SM}|$ is around 1 for the LH and SLH, but smaller than 1 for the LHT-A and LHT-B. In the LHT-A and LHT-B, the T-odd quarks further suppress the hgg coupling, and the suppression is equal compared with that of top quark and T quark. Note that the reduced $hb\bar{b}$ coupling can suppress the total width of

TABLE I. The detailed information of some samples in the LHT-A and LHT-B.

	LHT-B P1	LHT-B P2	LHT-A P3
f (GeV)	601.22	999.96	999.96
r	1.9326	1.9286	1.9286
χ^2	23.63	20.76	22.09
M_T	1044.27	1722.58	1722.58
M_{W_H}	370.47	624.92	624.92
M_Φ	427.41	717.19	717.19
M_{A_H}	82.85	148.54	148.54
$\lvert C_{hgg}/\mathrm{SM}\rvert^2$	0.5475	0.8265	0.8265
$\lvert C_{hbb}/\mathrm{SM}\rvert^2$	0.6013	0.8505	0.9715
$\lvert C_{h\tau\tau}/\mathrm{SM}\rvert^2$	0.6013	0.8505	0.9715
$\lvert C_{h\gamma\gamma}/\mathrm{SM}\rvert^2$	0.9531	0.9817	0.9817
$\lvert C_{hWW}/\mathrm{SM}\rvert^2$	0.9162	0.9697	0.9697
$\lvert C_{hZZ}/\mathrm{SM}\rvert^2$	0.9162	0.9697	0.9697
$\lvert C_{htt}/\mathrm{SM}\rvert^2$	0.8255	0.9322	0.9322
LHC, ggF + ttH, $\gamma\gamma$	0.763	0.921	0.847
LHC, VBF + VH, $\gamma\gamma$	1.278	1.080	0.994
Tev, inclusive, $\gamma\gamma$	0.877	0.956	0.880
LHC, inclusive, ZZ^*	0.797	0.929	0.855
LHC, WW^*, $e\nu\mu\nu$	0.759	0.917	0.844
LHC, 0/1 jet, WW^*	0.749	0.914	0.841
LHC, VBF tag, WW^*	1.144	1.040	0.957
LHC, VH tag, WW^*	1.228	1.067	0.982
Tev, inclusive, WW^*	0.843	0.944	0.869
LHC, VH tag, $b\bar{b}$	0.806	0.936	0.984
LHC, ttH tag, $b\bar{b}$	0.726	0.900	0.946
Tev, VH tag, $b\bar{b}$	0.806	0.936	0.984
LHC, ggF, $\tau\tau$	0.482	0.798	0.839
LHC, VBF + VH, $\tau\tau$	0.806	0.936	0.984
LHC, 0/1 jet, $\tau\tau$	0.559	0.831	0.873
LHC, VBF tag, $\tau\tau$	0.744	0.910	0.956
LHC, VH tag, $\tau\tau$	0.806	0.936	0.984

the 125.5 GeV Higgs boson, which helps to enhance the branching ratios of $h \to \gamma\gamma, WW^*, ZZ^*, \tau\bar{\tau}$. However, the reduced hgg coupling suppresses the cross section of $gg \to h$ more sizably and the reduced couplings $h\gamma\gamma, hWW, hZZ$, and $h\tau\bar{\tau}$ suppress the width of $h \to \gamma\gamma, WW^*, ZZ^*, \tau\bar{\tau}$. Besides, the total width of the Higgs boson in the SLH is enhanced by the new decay modes $h \to Z\eta$ and $h \to \eta\eta$ for a light η and thus the signal rates are reduced further.

Figures 4 and 5 show that the Higgs couplings of LHT-B can be very different from those of the SM, which can lead to some interesting Higgs phenomena at the collider. Therefore, we will pay special attention to this model in the following discussions, and the LHT-A is also comparatively considered.

In Fig. 6 we show the exclusive diphoton signal rates from the $VBF + VH$ and $ggF + ttH$ channels. We can see that, although the Higgs couplings and inclusive diphoton rate are always reduced, the exclusive rate of $VBF + VH$ can be enhanced in the LHT-B. The reason is that the $hb\bar{b}$

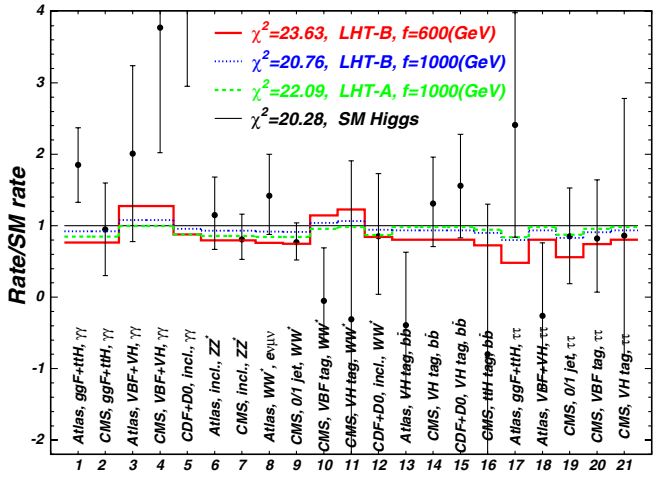

FIG. 7 (color online). Predictions of some samples for various Higgs signal rates at the LHC and Tevatron, compared with the SM values and the experimental data. The experiment data are taken from Ref. [26].

coupling in the LHT-B is suppressed sizably, which greatly enhances the branching ratio of $h \to \gamma\gamma$. Therefore, the LHT-B is favored by the enhanced exclusive diphoton data of $VBF + VH$ from ATLAS and CMS (note that the data have a rather large uncertainty).

Now we take some benchmark points in the LHT-A and LHT-B to demonstrate the Higgs properties in Table I and Fig. 7. We see that in the LHT-A all the signal rates are suppressed while in the LHT-B the exclusive signal rates (except $h \to b\bar{b}$ and $h \to \tau\bar{\tau}$) of $VBF + VH$ are enhanced, especially for a small f. Compared to the experimental data shown in Fig. 7, we find that the LHT-B can provide a better fit than the SM for some channels like $VBF + VH$, $\gamma\gamma$ of ATLAS and CMS, *inclusive* ZZ^*, $0/1$ *jet*, WW^*, $\tau\tau$ data of CMS.

IV. CONCLUSION

In this paper we compared the properties of the SM-like Higgs boson predicted by the typical little Higgs models (namely, the LH, LHT-A, LHT-B, and SLH) with the latest LHC Higgs search data. For a SM-like Higgs boson around 125.5 GeV, we obtained the following observations: (i) In these models the inclusive diphoton signal rates cannot be enhanced and lie outside the 2σ range of the present data. (ii) While most signal rates are suppressed in these models, some exclusive signal rates in the VBF and VH channels can be enhanced in the LHT-B. (iii) Compared with the SM, these models provide no better global fit to the whole data set, but for some special channels a better fit can be obtained, especially in the LHT-B. (iv) In these models the Higgs couplings are suppressed and approach the SM values for a sufficiently large-scale f.

We should stress again that in little Higgs models the inclusive diphoton rate cannot be enhanced for some obvious reasons. In these models the T quark (top quark partner) and new heavy gauge bosons are responsible for canceling the one-loop quadratic divergence of the Higgs mass contributed by the top quark and SM gauge bosons, respectively. As a result, the Higgs couplings to top quark and T quark have opposite sign, and the contributions of the T-quark loop will reduce the effective hgg coupling. Similarly, the Higgs couplings to the W boson and the heavy charged gauge boson have opposite sign, and the contributions of the heavy charged gauge boson loop will reduce the effective $h\gamma\gamma$ coupling. In addition, with the expansion of the nonlinear sigma field, the Higgs couplings to the top quark and W boson are suppressed, which will further reduce the effective hgg and $h\gamma\gamma$ couplings. However, the $hb\bar{b}$ coupling is also reduced sizably in the LH, SLH, and LHT-B, and thus the signal rates in some channels are quite close to the SM values.

The future LHC Higgs data (especially the diphoton rate) with large statistics will allow for a critical test for these little Higgs models. If the enhancement of the diphoton rate persists or gets enlarged, the little Higgs models will be strongly disfavored or excluded. Otherwise, if the rate drops below the SM value, these models will be favored. Also, these models have other correlated phenomenology like the enhanced Higgs pair production [29,38] and the suppressed $ht\bar{t}$ production [39] at the LHC. All this phenomenology can be jointly utilized to test the little Higgs models and distinguish them from other new physics models.

ACKNOWLEDGMENTS

This work was supported by the National Natural Science Foundation of China (NNSFC) under Grants No. 11105116, No. 11005089, No. 11275245, No. 10821504, No. 11135003, and No. 11175151.

Note added.—When this manuscript was being prepared, a paper with similar analysis and similar results appeared in the arXiv [40].

[1] N. Arkani-Hamed, A. G. Cohen, and H. Georgi, Phys. Lett. B **513**, 232 (2001); N. Arkani-Hamed, A. G. Cohen, E. Katz, A. E. Nelson, T. Gregoire, and J. G. Wacker, J. High Energy Phys. 08 (2002) 021.

[2] D. E. Kaplan and M. Schmaltz, J. High Energy Phys. 10 (2003) 039; I. Low, W. Skiba, and D. Smith, Phys. Rev. D **66**, 072001 (2002); S. Chang and J. G. Wacker, Phys. Rev. D **69**, 035002 (2004); T. Gregoire, D. R. Smith, and J. G.

Wacker, Phys. Rev. D **69**, 115008 (2004); W. Skiba and J. Terning, Phys. Rev. D **68**, 075001 (2003); S. Chang, J. High Energy Phys. 12 (2003) 057; H. Cai, H.-C. Cheng, and J. Terning, J. High Energy Phys. 05 (2009) 045; A. Freitas, P. Schwaller, and D. Wyler, J. High Energy Phys. 12 (2009) 027; R. Barcelo and M. Masip, Phys. Rev. D **78**, 095012 (2008); M. Schmaltz, D. Stolarski, and J. Thaler, J. High Energy Phys. 09 (2010) 018.

[3] N. Arkani-Hamed, A. G. Cohen, E. Katz, and A. E. Nelson, J. High Energy Phys. 07 (2002) 034.

[4] M. Schmaltz, J. High Energy Phys. 08 (2004) 056.

[5] T. Han, H. E. Logan, and L. T. Wang, J. High Energy Phys. 01 (2006) 099.

[6] C. Csaki, J. Hubisz, G. Kribs, P. Meade, and J. Terning, Phys. Rev. D **67**, 115002 (2003); **68**, 035009 (2003); J. L. Hewett, F. J. Petriello, and T. G. Rizzo, J. High Energy Phys. 10 (2003) 062; M. C. Chen and S. Dawson, Phys. Rev. D **70**, 015003 (2004); M. C. Chen, Mod. Phys. Lett. A **21**, 621 (2006).

[7] H. C. Cheng and I. Low, J. High Energy Phys. 09 (2003) 051.

[8] H. C. Cheng and I. Low, J. High Energy Phys. 08 (2004) 061; I. Low, J. High Energy Phys. 10 (2004) 067.

[9] CMS Collaboration, Phys. Lett. B **716**, 30 (2012).

[10] ATLAS Collaboration, Phys. Lett. B **716**, 1 (2012).

[11] TEVNPH Working Group for the CDF and D0 Collaborations, arXiv:1207.0449.

[12] ATLAS Collaboration, Note Report No. ATLAS-CONF-2012-170.

[13] CMS Collaboration, Note Report No. CMS-PAS-HIG-12-045.

[14] ATLAS Collaboration, Note Report No. ATLAS-CONF-2012-168.

[15] ATLAS Collaboration, Note Report No. ATLAS-CONF-2012-169.

[16] CMS Collaboration, Note Report No. CMS-PAS-HIG-12-041.

[17] The Higgs diphoton rate can be enhanced in some popular supersymmetry models; see, e.g., M. Carena, S. Gori, N. R. Shah, and C. E. M. Wagner, J. High Energy Phys. 03 (2012) 014; M. Carena, S. Gori, N. R. Shah, C. E. M. Wagner, and L.-T. Wang, J. High Energy Phys. 07 (2012) 175; J. Cao, Z. Heng, J. M. Yang, and J. Zhu, J. High Energy Phys. 10 (2012) 079; J. Cao, Z. Heng, J. M. Yang, Y. Zhang, and J. Zhu, J. High Energy Phys. 03 (2012) 086; J. Cao, Z. Heng, D. Li, and J. M. Yang, Phys. Lett. B **710**, 665 (2012); J. Cao, Z. Heng, T. Liu, and J. M. Yang, Phys. Lett. B **703**, 462 (2011); U. Ellwanger, J. High Energy Phys. 03 (2012) 044; U. Ellwanger and C. Hugonie, Adv. High Energy Phys. **2012**, 625389 (2012); A. Arbey, M. Battaglia, A. Djouadi, and F. Mahmoudi, J. High Energy Phys. 09 (2012) 107; K. Hagiwara, J. S. Lee, and J. Nakamura, J. High Energy Phys. 10 (2012) 002; R. Benbrik, M. G. Bock, S. Heinemeyer, O. Stål, G. Weiglein, and L. Zeune, Eur. Phys. J. C **72**, 2171 (2012); N. Christensen, T. Han, and S. Su, Phys. Rev. D **85**, 115018 (2012); T. Cheng, arXiv:1207.6392; B. Kyae and J.-C. Park, arXiv:1207.3126; H. An, T. Liu, and L.-T. Wang, Phys. Rev. D **86**, 075030 (2012); J. F. Gunion, Y. Jiang, and S. Kraml, Phys. Rev. D **86**, 071702 (2012); J. Ke, M.-X. Luo, L.-Y. Shan, K. Wang, and L. Wang, Phys. Lett. B **718**, 1334 (2013); G. Belanger, U. Ellwanger, J. F. Gunion, Y. Jiang, and S. Kraml, arXiv:1208.4952; M. Drees, Phys. Rev. D **86**, 115018 (2012); S. F. King, M. Muhlleitner, R. Nevzorov, and K. Walz, Nucl. Phys. **B870**, 323 (2013); K. Choi, S. H. Im, K. S. Jeong, and M. Yamaguchi, J. High Energy Phys. 02 (2013) 090; M. Berg, I. Buchberger, D. M. Ghilencea, and C. Petersson, arXiv:1212.5009; L. Aparicio, P. G. Cámara, D. G. Cerdeño, L. E. Ibáñez, and I. Valenzuela, J. High Energy Phys. 02 (2013) 084; C. Balazs and S. K. Gupta, Phys. Rev. D **87**, 035023 (2013); K. Cheung, C.-T. Lu, and T.-C. Yuan, arXiv:1212.1288.

[18] C. Haluch and R. Matheus, Phys. Rev. D **85**, 095016 (2012); X.-G. He, B. Ren, and J. Tandean, Phys. Rev. D **85**, 093019 (2012); A. Arhrib, R. Benbrik, and C.-H. Chen, arXiv:1205.5536; E. Cervero and J.-M. Gerard, Phys. Lett. B **712**, 255 (2012); L. Wang and X.-F. Han, J. High Energy Phys. 05 (2012) 088; A. Drozd, B. Grzadkowski, J. F. Gunion, and Y. Jiang, arXiv:1211.3580; S. Chang, S. K. Kang, J.-P. Lee, K. Y. Lee, S. C. Park, and J. Song, arXiv:1210.3439; N. Chen and H.-J. He, J. High Energy Phys. 04 (2012) 062; T. Abe, N. Chen, and H.-J. He, J. High Energy Phys. 01 (2013) 082; C. Han, N. Liu, L. Wu, J. M. Yang, and Y. Zhang, arXiv:1212.6728.

[19] A. G. Akeroyd and S. Moretti, Phys. Rev. D **86**, 035015 (2012); A. Arhrib, R. Benbrik, M. Chabab, G. Moultaka, and L. Rahili, J. High Energy Phys. 04 (2012) 136; L. Wang and X.-F. Han, Phys. Rev. D **86**, 095007 (2012); **87**, 015015 (2013).

[20] G. Blanger, A. Belyaev, M. Brown, M. Kakizaki, and A. Pukhov, EPJ Web Conf. **28**, 12070 (2012); K. Cheung and T.-C. Yuan, Phys. Rev. Lett. **108**, 141602 (2012).

[21] Y. Cai, W. Chao, and S. Yang, J. High Energy Phys. 12 (2012) 043; S. Chang, C. A. Newby, N. Raj, and C. Wanotayaroj, Phys. Rev. D **86**, 095015 (2012); J. Berger, J. Hubisz, and M. Perelstein, J. High Energy Phys. 07 (2012) 016; S. Dawson and E. Furlan, Phys. Rev. D **86**, 015021 (2012); S. Dawson, E. Furlan, and I. Lewis, Phys. Rev. D **87**, 014007 (2013); M. Chala, J. High Energy Phys. 01 (2013) 122.

[22] L. Wang and J. M. Yang, Phys. Rev. D **84**, 075024 (2011); **79**, 055013 (2009).

[23] T. Han, H. E. Logan, B. McElrath, and L.-T. Wang, Phys. Rev. D **67**, 095004 (2003); H. E. Logan, Phys. Rev. D **70**, 115003 (2004).

[24] T. Han, H. E. Logan, B. McElrath, and L.-T. Wang, Phys. Lett. B **563**, 191 (2003).

[25] C. R. Chen, K. Tobe, and C. P. Yuan, Phys. Lett. B **640**, 263 (2006).

[26] G. Belanger, B. Dumont, U. Ellwanger, J. F. Gunion, and S. Kraml, J. High Energy Phys. 02 (2013) 053.

[27] J. Hubisz and P. Meade, Phys. Rev. D **71**, 035016 (2005).

[28] K. Cheung and J. Song, Phys. Rev. D **76**, 035007 (2007).

[29] X.-F. Han, L. Wang, and J. M. Yang, Nucl. Phys. **B825**, 222 (2010).

[30] S. Chang and H.-J. He, Phys. Lett. B **586**, 95 (2004); E. Katz, J. Lee, A. E. Nelson, and D. G. E. Walker, J. High Energy Phys. 10 (2005) 088; F. Bazzocchi, M. Fabbrichesi, and M. Piai, Phys. Rev. D **72**, 095019 (2005).

[31] A. Djouadj, J. Kalinowski, and M. Spira, Comput. Phys. Commun. **108**, 56 (1998).

[32] J. Hubisz, P. Meade, A. Noble, and M. Perelstein, J. High Energy Phys. 01 (2006) 135.

[33] J. I. Illana and M. D. Jenkins, Acta Phys. Pol. B **40**, 3143 (2009); F. d. Aguila, J. I. Illana, and M. D. Jenkins, Nucl. Phys. B, Proc. Suppl. **205–206**, 158 (2010).

[34] F. d. Aguila, J. I. Illana, and M. D. Jenkins, J. High Energy Phys. 03 (2011) 080.

[35] W.-M. Yao *et al.* (Particle Data Group), J. Phys. G **33**, 1 (2006); R. Balest *et al.* (CLEO Collaboration), Phys. Rev. D **51**, 2053 (1995).

[36] J. R. Espinosa, C. Grojean, M. Muhlleitner, and M. Trott, J. High Energy Phys. 05 (2012) 097; 12 (2012) 045.

[37] P. P. Giardino, K. Kannike, M. Raidal, and A. Strumia, J. High Energy Phys. 06 (2012) 117; Phys. Lett. B **718**, 469 (2012).

[38] J.-J. Liu, W.-G. Ma, G. Li, R.-Y. Zhang, and H.-S. Hou, Phys. Rev. D **70**, 015001 (2004); C. O. Dib, R. Rosenfeld, and A. Zerwekh, J. High Energy Phys. 05 (2006) 074; L. Wang, W. Wang, J. Yang, and H. Zhang, Phys. Rev. D **76**, 017702 (2007); L. Wang and J. Yang, Phys. Rev. D **77**, 015020 (2008).

[39] L. Wang, W. Wang, J. Yang, and H. Zhang, Phys. Rev. D **75**, 074006 (2007).

[40] J. Reuter and M. Tonini, J. High Energy Phys. 02 (2013) 077.